

Reflection asymmetric relativistic mean field approach and its application to the octupole deformed nucleus ^{226}Ra

L. S. Geng^{1,2}, J. Meng^{1,2,3}, and H. Toki⁴

¹*School of Physics, Peking University, Beijing 100871*

²*Institute of Theoretical Physics, Chinese Academy of Sciences, Beijing 100080*

³*Center of Theoretical Nuclear Physics, National Laboratory of Heavy Ion Accelerator, Lanzhou 730000*

⁴*Research Center for Nuclear Physics(RCNP), Osaka University, Ibaraki 567-0047, Japan*

(Dated: October 24, 2018)

A Reflection ASymmetric Relativistic Mean Field (RAS-RMF) approach is developed by expanding the equations of motion for both the nucleons and the mesons on the eigenfunctions of the two-center harmonic-oscillator potential. The efficiency and reliability of the RAS-RMF approach are demonstrated in its application to the well-known octupole deformed nucleus ^{226}Ra and the available data, including the binding energy and the deformation parameters, are well reproduced.

PACS numbers: 21.60.-n; 21.60.Jz; 21.10.Ft; 21.10.Gv

The relativistic mean field (RMF) model is one of the most successful microscopic models in nuclear physics. It incorporates from the beginning very important relativistic effects, such as the existence of two types of potentials (Lorentz scalar and four-vector) and the resulting strong spin-orbit interaction [1, 2]. During the past two decades, it has received wide attention due to its successes in describing many nuclear phenomena for stable nuclei, exotic nuclei, as well as supernovae and neutron stars [1, 2]. Recently, a systematic theoretical study of over 7000 nuclei has been performed in the RMF model and overall good agreements with existing data were obtained [3]. To solve the RMF equations for finite systems, in particular deformed systems, the basis expansion method is most widely employed [4, 5, 6], though other alternatives exist [7, 8, 9, 10]. The basis expansion method is very efficient, and, more importantly, very intuitive. Due to the limitation of the conventional harmonic-oscillator potential (spherical, axial, or triaxial), reflection symmetry is always assumed in these methods [4, 5].

On the other hand, as early as in the 1950s, it was realized that some nuclei may have a shape asymmetric under reflection, such as a pear shape [11], with the observation of low-lying 1^- states in the actinide nuclei [12, 13, 14]. Microscopically, this is attributed to the coupling between single-particle states which differ by $\Delta\ell = 3$ and $\Delta j = 3$. These states lie close to each other and to the Fermi surface at proton and neutron numbers near 34, 56, 88 and neutron number near 134, where octupole correlations are expected to be the strongest [15]. Octupole deformation increases the nuclear binding energy by only a few MeV for most cases, but it is essential to explain a lot of experimental observations [15], such as the appearance of parity doublets [16]. It can also lower the second fission-barrier of heavy and superheavy nuclei and explain the asymmetric mass distribution observed in the fission of ^{240}Pu [7].

In the present work, we develop a Reflection ASymmetric Relativistic Mean Field (RAS-RMF) approach so that nuclei having reflection-asymmetric shapes can be studied (We nevertheless assume axial symmetry). To

achieve this and to follow the general principle of the basis expansion technique [4, 17], we employ the eigenfunctions of the two-center harmonic-oscillator (TCHO) potential, which was traditionally used in the two-center shell model (TCSM) by the Frankfurt group [18, 19]. The TCHO basis has been widely used in studies of fission, fusion, heavy-ion emission, and various cluster phenomena studies [20]. Its applications in microscopic mean-field models, however, are very rare except a few in non-relativistic Hartree-Fock models in the 1970s [21, 22].

The RMF model used here is the standard one and its detailed reviews can be found in Refs. [1, 2]; therefore, only a brief introduction is provided in the following. The adopted Lagrangian density is

$$\begin{aligned} \mathcal{L} = & \bar{\psi}(i\gamma^\mu\partial_\mu - M)\psi \\ & + \frac{1}{2}\partial_\mu\sigma\partial^\mu\sigma - \frac{1}{2}m_\sigma^2\sigma^2 - \frac{1}{3}g_2\sigma^3 - \frac{1}{4}g_3\sigma^4 - g_\sigma\bar{\psi}\sigma\psi \\ & - \frac{1}{4}\Omega_{\mu\nu}\Omega^{\mu\nu} + \frac{1}{2}m_\omega^2\omega_\mu\omega^\mu + \frac{1}{4}c_4(\omega_\mu\omega^\mu)^2 - g_\omega\bar{\psi}\gamma^\mu\psi\omega_\mu \\ & - \frac{1}{4}R^a{}_{\mu\nu}R^{a\mu\nu} + \frac{1}{2}m_\rho^2\rho^a\rho^a - g_\rho\bar{\psi}\gamma_\mu\tau^a\psi\rho^{\mu a} \\ & - \frac{1}{4}F_{\mu\nu}F^{\mu\nu} - e\bar{\psi}\gamma_\mu\frac{1-\tau_3}{2}A^\mu\psi, \end{aligned} \quad (1)$$

where all symbols have their usual meanings. Using the classical variational principle, one can obtain the Dirac equation for the nucleons and Klein-Gordon equations for the mesons [1, 2]. To solve these equations, we employ the basis expansion method, which has been widely used in both non-relativistic and relativistic mean-field models [4, 17]. For axial-symmetric reflection-asymmetric systems, the spinors f_i^\pm and g_i^\pm can be expanded in terms of the eigenfunctions of the TCHO potential

$$V(r_\perp, z) = \frac{1}{2}M\omega_\perp^2 r_\perp^2 + \begin{cases} \frac{1}{2}M\omega_1^2(z+z_1)^2, & z < 0 \\ \frac{1}{2}M\omega_2^2(z-z_2)^2, & z \geq 0 \end{cases}, \quad (2)$$

where M is the nucleon mass, z_1 and z_2 (real, positive) represent the distances between the centers of the spheroids and their intersection plane, and $\omega_1(\omega_2)$

TABLE I: Convergences of the RAS-RMF calculations versus the number of shells $N(= N_F = N_B)$ for the ground-state properties of ^{16}O and ^{208}Pb , in comparison with those of the axial deformed RMF calculations [4].

^{16}O												
N	Binding energy per nucleon (MeV)						Charge radius (fm)					
	10	12	14	16	18	20	10	12	14	16	18	20
Axial deformed RMF	8.052	8.050	8.051	8.051	8.051	8.051	2.724	2.725	2.727	2.727	2.728	2.728
RAS-RMF	8.052	8.050	8.051	8.051	8.051	8.051	2.724	2.725	2.727	2.727	2.728	2.728
^{208}Pb												
N	Binding energy per nucleon (MeV)						Charge radius (fm)					
	10	12	14	16	18	20	10	12	14	16	18	20
Axial deformed RMF	7.837	7.896	7.896	7.888	7.887	7.886	5.515	5.517	5.509	5.512	5.516	5.515
RAS-RMF	7.852	7.891	7.891	7.886	7.886	7.884	5.523	5.510	5.510	5.516	5.517	5.516

TABLE II: Ground-state properties of ^{226}Ra , including the binding energy E_B , the quadrupole, octupole, and hexadecapole deformation parameters for neutron, proton(charge), and matter density distributions ($\beta_{\ell n}$, $\beta_{\ell p(c)}$) and β_ℓ with $\ell = 2, 3$, and 4) obtained from the RAS-RMF and axial deformed RMF calculations, in comparison with the data.

	β_{2n}	$\beta_{2p(c)}$	β_2	β_{3n}	$\beta_{3p(c)}$	β_3	β_{4n}	$\beta_{4p(c)}$	β_4	E_B [MeV]
Axial deformed RMF	0.19	0.18	0.19	–	–	–	0.14	0.12	0.13	1729.1
RAS-RMF	0.21	0.20	0.21	-0.16	-0.15	-0.16	0.17	0.15	0.16	1731.8
Exp.		0.20			-0.13					1731.6

are the corresponding oscillator frequencies for $z < 0$ ($z \geq 0$) [18, 19, 24].

Imposing the assumption of volume-surface conservation [18, 19, 24], the TCHO basis can be completely specified by three parameters: δ_2 , the quadrupole deformation parameter of the $z > 0$ half spheroid which defines the ratio of ω_2 and ω_\perp through $\frac{\omega_2}{\omega_\perp} = \exp(-\frac{3}{2}\sqrt{\frac{5}{4\pi}}\delta_2)$ [4]; δ_3 , which defines the ratio of ω_1 and ω_2 through $\delta_3 = \frac{\omega_1}{\omega_2}$; and $\Delta z = z_1 + z_2$, the distance between the two centers. Here, the spherical harmonic-oscillator parameters are chosen as $\hbar\omega_0 = 41A^{-1/3}$ and $R_0 = 1.2A^{1/3}$ as in Refs. [4, 17, 18, 19]. Since the primary purpose of the present work is to extend the RMF model to reflection-asymmetric systems, only the δ_3 degree of freedom of the TCHO basis is explored while the Δz degree of freedom will be left for future studies, i.e. we set $\Delta z \approx 0$.

For $\delta_3 = 1.0$ and $\Delta z \approx 0$, the TCHO potential reduces to the reflection-symmetric harmonic-oscillator potential and the RAS-RMF method becomes equivalent to the axial deformed RMF approach developed in Ref. [4]. In Table I, the results obtained from the RAS-RMF calculations are compared with those obtained from the axial deformed RMF calculations for ^{16}O and ^{208}Pb . The mean-field force employed is NL3 [25]. Using other forces, such as NL1 [26], does not influence our conclusion here. As expected, the agreement between these two calculations is remarkable. This demonstrates the equivalence of these two codes in the special case. Ta-

ble I also shows that the results already converge at $N(= N_F = N_B) = 16$ even for ^{208}Pb . In the following, unless indicated otherwise, numerical calculations will be performed by using $N = 16$. For $\delta_3 \neq 1.0$, one should note that the eigenvalues of $\phi_\nu(z)$, ν_1 and ν_2 , are not integers anymore. Therefore, in this case, the dimension of the basis (denoted by \tilde{N}) is chosen to be the same as that at $\delta_3 = 1.0$ (denoted by N).

In the following, we apply the RAS-RMF approach to the nucleus ^{226}Ra , which has been predicted to have a reflection-asymmetric ground state by various theoretical models (see Ref. [7] and references therein). The purpose is to demonstrate the validity of the RAS-RMF approach. For the mean-field channel, two effective forces have been used, i.e NL3 [25] and NL1 [26]. The numerical results obtained from these two forces turn out to be quite similar for ^{226}Ra , in particular for the deformation parameters. Therefore, only the numerical results obtained with NL1 are presented. For the pairing channel, the constant gap approach with $\Delta = 11.2 \text{ MeV}/\sqrt{A}$ is used.

On the upper panel of Fig. 1, the potential energy surfaces of ^{226}Ra obtained from RAS-RMF and axial deformed RMF calculations are plotted as functions of the quadrupole deformation parameter β_2 . These are obtained by a quadratic constraint on the quadrupole moment $\langle Q_2 \rangle = \langle r^2 Y_{20} \rangle$ [27] while the octupole deformations have been left free to adjust themselves to the min-

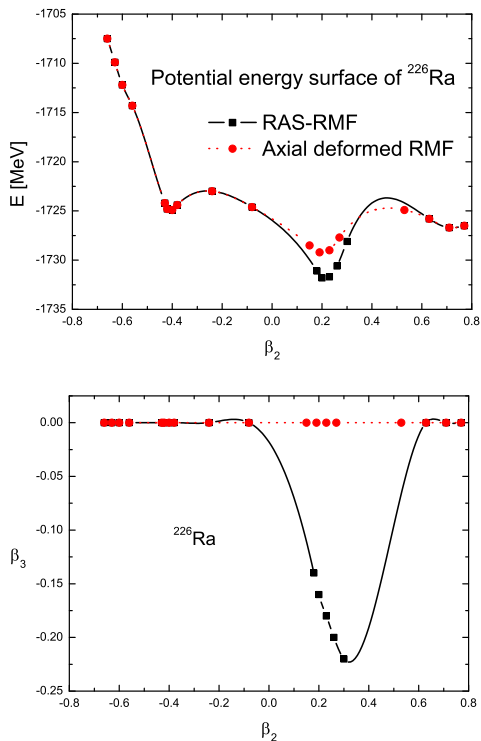


FIG. 1: Upper panel: the potential energy surfaces of ^{226}Ra as versus the quadrupole deformation parameter β_2 ; lower panel: the octupole deformation parameter β_3 of ^{226}Ra as a function of β_2 obtained from the RAS-RMF calculations.

imum configuration. It is easily seen that the asymmetric ground state is lower than the symmetric ground state by roughly 3 MeV while the asymmetric barrier at $\beta_2 \approx 0.5$ is slightly higher than the corresponding symmetric barrier. For the other parts of the potential energy surfaces, these two calculations agree with each other. It should be mentioned that all these are in coincidence with the results of Ref. [7]. Naturally, one would think that the above differences originate from the octupole degree of freedom, which is in fact the case as can be seen from the lower panel of Fig. 1.

In Table II, the ground-state properties of ^{226}Ra obtained from RAS-RMF and axial deformed RMF calculations are tabulated. It is clearly seen that (i) the asymmetric ground state is more bound by roughly 2.7 MeV than the symmetric ground state, (ii) the quadrupole and hexadecapole deformations obtained from the RAS-RMF calculations are slightly larger than those from the axial deformed RMF calculations due to the emergence of octupole deformation, and (iii) the slight difference between the neutron octupole deformation and the proton octupole deformation would generate a non-vanishing

static electric dipole moment [7]. The experimental binding energy of ^{226}Ra is 1731.6 MeV [28], which agrees well with our RAS-RMF prediction, 1731.8 MeV (see Table II). Experimentally, the charge quadrupole and octupole deformation parameters can be extracted from the experimental $B(E2) \uparrow$ [29] and $B(E3) \uparrow$ [15] values by

$$\beta_{2c} = \frac{4\pi}{3ZR_0^2} \left[\frac{B(E2) \uparrow}{e^2} \right]^{1/2}, \quad \beta_{3c} = \frac{4\pi}{3ZR_0^3} \left[\frac{B(E3) \uparrow}{e^2} \right]^{1/2}. \quad (3)$$

From $B(E2) \uparrow$ of $5.1514 b^2 e^2$ [29] and $B(E3) \uparrow$ of $1.1011 b^3 e^2$ [30] for ^{226}Ra , one can deduce the corresponding β_2 and β_3 to be 0.20 and 0.13, respectively, which agree well with our predictions as what can be seen from Table II. It should be noted that our calculations are symmetric for $\beta_3 > 0$ and $\beta_3 < 0$. Therefore, in Table II, the experimental β_3 is chosen to have a negative sign.

The nuclear shape can be visualized from its density distributions. In Fig. 2, the neutron and proton density distributions of the ground state of ^{226}Ra obtained from the axial deformed RMF calculations and those obtained from our RAS-RMF calculations are plotted as functions of z and y on the $x = 0$ plane. It is easily seen that the ground state in the axial deformed RMF calculations corresponds to a nucleus of a spheroid shape while the ground state in our RAS-RMF calculations corresponds to a nucleus of a pear shape. It is noticed that the neutron density at the center of the nucleus is larger than the corresponding proton density due to the larger number of neutrons as compared to that of protons.

In summary, we have solved the RMF equations for axial-symmetric reflection-asymmetric systems, i.e. we have developed the RAS-RMF approach. The numerical details of this approach are presented. It is then applied to investigate the ground-state properties of ^{226}Ra and good agreements with existing data are obtained. The RAS-RMF approach, therefore, provides another microscopic framework to study nuclei with intrinsic reflection-asymmetric shapes and the rich nuclear phenomena related [15]. A nonzero atomic electric-dipole moment (EDM) would signify time-reversal violation from outside the Standard Model; while EDMs are enhanced in atoms that have octupole deformed nuclei, such as ^{225}Ra [31]. This can be studied in the future within the RAS-RMF framework. This approach with the Δz degree of freedom may also be useful in studies of largely deformed systems, for example, those during fission or fusion.

We thank E. G. Zhao, S.-G. Zhou, and H. F. Lü for stimulating discussions. This work is supported in part by the National Natural Science Foundation of China under Grant Nos. 10435010, 10221003, and the Doctoral Program Foundation from the Ministry of Education in China.

[1] Ring P 1996 Prog. Part. Nucl. Phys. 37, 193.

[2] Meng J, Toki H, Zhou S G, Zhang S Q, Long W H and

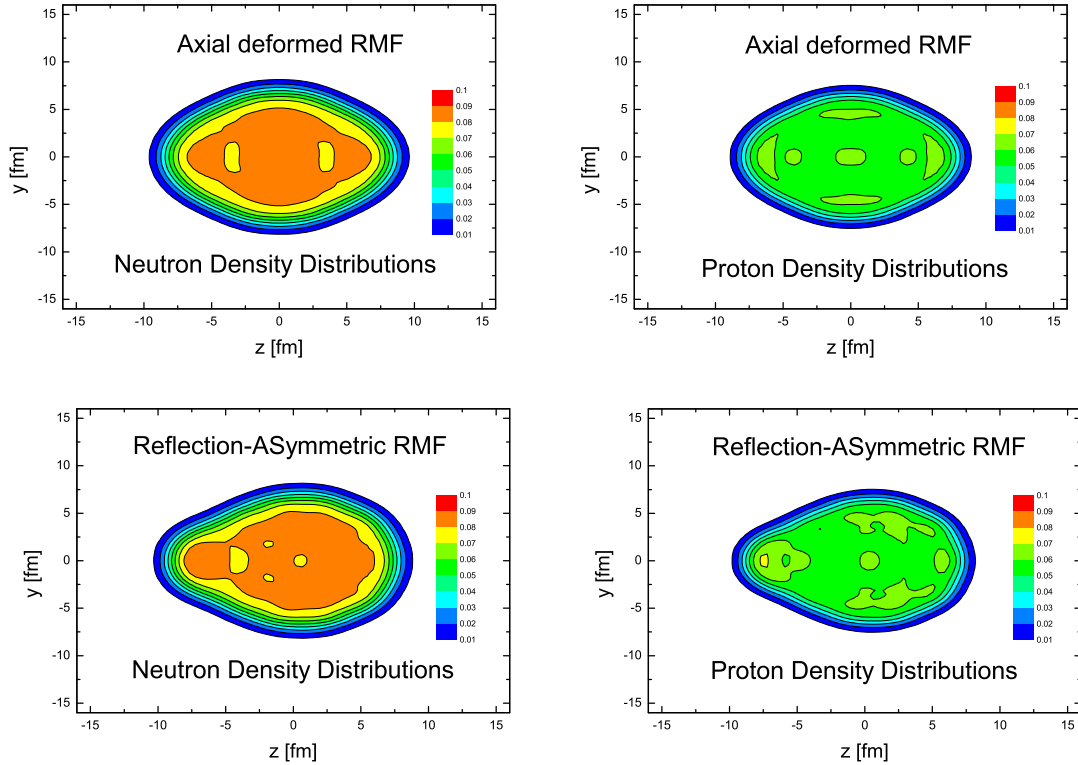


FIG. 2: Neutron and proton density distributions of the ground state of ^{226}Ra versus z and y on the $x = 0$ plane. Upper panel: results obtained from the axial deformed RMF calculations; lower panel: results obtained from the RAS-RMF calculations.

- Geng L S 2005 Prog. Part. Nucl. Phys. 57, 470.
- [3] Geng L S , Toki H and Meng J 2005 Prog. Theor. Phys. 113, 785.
- [4] Ring P, Gambhir Y K and Lalazissis G A 1997 Comput. Phys. Commun. 105, 77.
- [5] Hirata D, Sumiyoshi K, Carlson B V, Toki H and Tanihata I 1996 Nucl. Phys. A 609, 131.
- [6] Meng J, Peng J, Zhang S Q and Zhou S G 2006 Phys. Rev. C 73, 037303.
- [7] Rutz K, Maruhn J A, Reinhard P G and Greiner W 1995 Nucl. Phys. A 590, 680.
- [8] Meng J 1998 Nucl. Phys. A 635, 3.
- [9] Pöschl W 1998 Comput. Phys. Commun. 112, 42.
- [10] Zhou S G , Meng J and Ring P 2003 Phys. Rev. C 68, 034323.
- [11] Lee K and Inglis D R 1957 Phys. Rev. 108, 774.
- [12] Asaro F, Stephens F Jr. and Perlman I 1953 Phys. Rev. 92, 1495.
- [13] Stephens F Jr., Asaro F and Perlman I 1954 Phys. Rev. 96, 1568.
- [14] Stephens F Jr., Asaro F and Perlman I 1955 Phys. Rev. 100, 1543.
- [15] Butler P A and Nazarewicz W 1996 Rev. Mod. Phys. 68, 349.
- [16] Chasman R R 1980 Phys. Lett. B 96, 7.
- [17] Vautherin D 1973 Phys. Rev. C 7, 296.
- [18] Holzer P, Mosel U and Greiner W 1969 Nucl. Phys. A 138, 241.
- [19] Maruhn J and Greiner W 1972 Z. Phys. 251, 431.
- [20] Greiner W, Park J Y and Scheid W 1994 Nuclear Molecules (World Scientific, Singapore).
- [21] Passler K H, Zint P G and Mosel U 1973 Phys. Lett. B 47, 419.
- [22] Dreizler R M , Galbraith H and Lin L 1974 Nucl. Phys. A 234, 253.
- [23] Geng L S, Toki H, Sugimoto S and Meng J 2003 Prog. Theor. Phys. 110, 921.
- [24] Mirea M 1996 Phys. Rev. C 54, 302.
- [25] Lalazissis G A, König J and Ring P 1997 Phys. Rev. C 55, 540.
- [26] Reinhard P G , Rufa M, Maruhn J A , Greiner W and Friedrich J 1986 Z. Phys. A 323, 13.
- [27] Flocard H, Quentin P, Kerman A K and Vautherin D 1973 Nucl. Phys. A 203, 433.
- [28] Audi G , Wapstra A H and Thibault C 2003 Nucl. Phys. A 729, 337.
- [29] Raman S , Nestor C W JR. and Tikkanen P 2001 At. Data Nucl. Data Tables 78, 1.
- [30] Wollersheim H J et al. 1993 Nucl. Phys. A 556, 261.
- [31] Dobaczewski J and Engel J 2005 Phys. Rev. Lett. 94, 232502.